PHYSICAL REVIEW D **87,** 036003 (2013)

Three Pomerons versus D0 and TOTEM data

V. A. Petrov[1,*] and A. Prokudin[2,†]

[1]*Division of Theoretical Physics, Institute for High Energy Physics, 142281 Protvino, Russia*
[2]*Jefferson Lab, 12000 Jefferson Avenue, Newport News, Virginia 23606, USA*

(Received 21 December 2012; published 6 February 2013)

This paper highlights the predictive power of the three-component Pomeron model designed by the authors ten years ago, with a partial account of the multiplicity of Pomerons in QCD. The model is put to the test by comparing its predictions with the recent data from the D0 and TOTEM collaborations at 1.96 and 7 TeV, respectively. We also compare model predictions for inelastic cross sections to experimental measurements by the TOTEM, CMS, ALICE, and ATLAS collaborations. It is shown that the D0 data are perfectly predicted by the model. Total, elastic, and inelastic cross-section predictions are in agreement with the measurements by the TOTEM, CMS, ALICE, and ATLAS collaborations. Differential cross-section data at 7 TeV show slight disagreement with predictions of the model in the high-t region. Discussions on the origin of the disagreement and conclusions are presented.

DOI: 10.1103/PhysRevD.87.036003 PACS numbers: 11.55.Jy, 13.60.Hb, 13.85.Hd, 13.85.Lg

I. INTRODUCTION

Publication of the D0 data [1] on elastic proton-antiproton scattering at $\sqrt{s} = 1.96$ TeV; TOTEM data [2–4] on elastic proton-proton differential scattering cross sections at $\sqrt{s} = 7$ TeV; and inelastic cross sections by the TOTEM [2], CMS [5,6], ALICE [7], and ATLAS collaborations [8] has triggered a great deal of interest in the diffractive community [9–25].

One of the striking features of the new data is that the predictions of the models [26–31] considered in Ref. [2], while often close to the measured experimental values, fail to predict the TOTEM data in detail. A compilation of these models was made in Ref. [31].

In this article, we would like to consider the model of Ref. [32], where predictions were made for the LHC at $\sqrt{s} = 14$ TeV, and to check the predictions of this model for D0 at $\sqrt{s} = 1.96$ TeV and the LHC (TOTEM) at $\sqrt{s} = 7$ TeV. We are going to use the parameters of the model fixed in Ref. [32] to ensure all our results are genuine predictions. One of the intrinsic ingredients of the model of Ref. [32] is a phenomenological account of the well-established fact that in theories with asymptotic freedom, there exist multiple leading Regge trajectories with intercepts that form an infinite set of numbers (independent of the coupling constant), accumulating near some minimum limit; see Ref. [33].

In massless QCD, the intercepts of the leading Pomeron set of trajectories behave as $\alpha_{\mathbb{P}_k} - 1 = \Delta_{\mathbb{P}_k} \propto \frac{\text{const}}{k}$ at $k \to \infty$. (See the second item in Ref. [33].) Up to now, no more detailed results have been derived rigorously from QCD, at least for the leading Pomeron trajectories. We should mention a recent attempt [34] based on some extra assumptions. Explicit formulas were obtained recently in Ref. [35] for (massless) quark-antiquark trajectories.

For the time being, we have decided to mimic the proliferation of Pomerons with a few (two, three, four, etc.) tentative trajectories, with all parameters to be phenomenologically defined by fitting the data. The best fit chooses the three-Pomeron option. Early attempts to use a two-component Pomeron model for a description of the total and inclusive cross sections can be found in Refs. [36–38]. It is worth mentioning a later attempt [39] to use a many-component QCD Pomeron model for description of the DIS data from HERA.

II. THE MODEL

Let us first briefly describe the model of the elastic scattering amplitude from Refs. [26,32]. The nuclear amplitude as a function of the impact parameter b is written in the eikonal form as

$$T^N(s, \vec{b}) = \frac{e^{2i\delta(s,\vec{b})} - 1}{2i}, \tag{1}$$

where the eikonal $\delta(s, b)$ is approximated by single-Reggeon exchanges:

$$\delta^{\bar{p}p}_{pp}(s, b) = \delta^{+}_{\mathbb{P}}(s, b) \mp \delta^{-}_{\mathbb{O}}(s, b) + \delta^{+}_{f}(s, b) \mp \delta^{-}_{\omega}(s, b). \tag{2}$$

We refer the reader to the original literature for details; let us simply recall that here $\delta^{+}_{\mathbb{P}}(s, b)$ denotes the Pomeron contributions, and the superscript "+" denotes C-even trajectories (the Pomeron trajectories have quantum numbers 0^+J^{++}), while "−" denotes C-odd trajectories. The term $\delta^{-}_{\mathbb{O}}(s, b)$ is the Odderon contribution (i.e., the C-odd partner of the Pomeron whose quantum numbers are 0^-J^{--}); $\delta^{+}_{f}(s, b)$ and $\delta^{+}_{\omega}(s, b)$ are the contributions of

*Vladimir.Petrov@ihep.ru
†prokudin@jlab.org

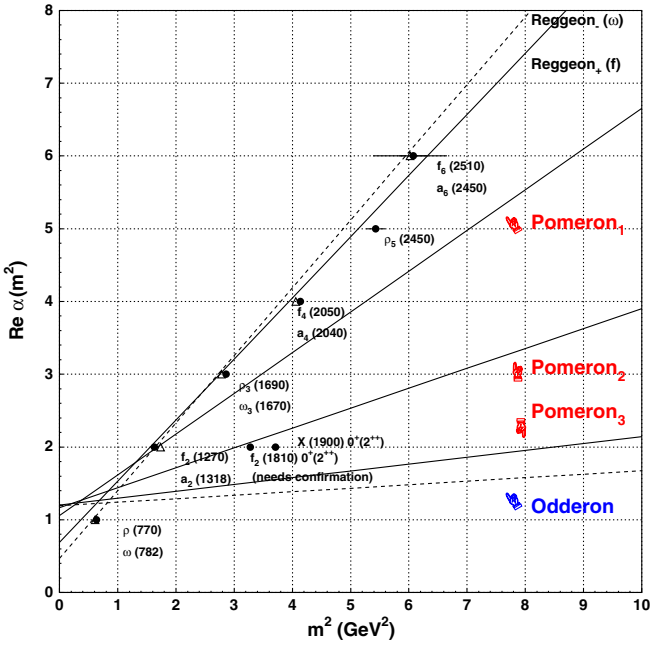

FIG. 1 (color online). Regge trajectories from Ref. [32].

secondary Reggeons, with f representative of the $C = +1$ families and ω of the $C = -1$ families.

This approximation for the eikonal is similar to the impact parameter approximation in quantum mechanics with single-Reggeon exchanges in the role of potentials. Actually, this assumption is generic for many models in the field. From the standpoint of the complex J plane, the eikonal has to have not only Regge poles, but generally more complicated singularities. Nonetheless, we believe that the pole approximation for the eikonal reasonably reflects the gross features of the diffractive hadron scattering. In our model, we use linear trajectories, and this could be justified if one considers only the low-t region. Our linear Pomeron trajectories can go below the line $J = 1$ at sufficiently large $-t$; however, Regge trajectories in QCD are nonlinear at negative t; see Ref. [40]. Pomeron trajectories most probably always lie higher than $J = 1$; see Ref. [41]. If there is a disagreement with data, we have to pay closer attention to such details.

As was said, the effective number of Pomerons was found to be three, and accordingly, the Pomeron contribution $\delta^+_{\mathbb{P}}(s, b)$ can be represented as the sum of three contributions:

$$\delta^+_{\mathbb{P}}(s, b) = \delta^+_{\mathbb{P}_1}(s, b) + \delta^+_{\mathbb{P}_2}(s, b) + \delta^+_{\mathbb{P}_3}(s, b), \qquad (3)$$

each of those having a particular Regge trajectory. Other models include complicated form factors [22] or a different type of singularity for the Pomeron [9].

Let us recall that if the form of Eq. (3) is indeed manifested in nature, then we expect to have particles lying on the corresponding trajectories. The model predicts $M^2_{\text{glueball}} = 1.68,\ 3.05,\ 8.51\ \text{GeV}^2$ for the 0^+2^{++} state. The trajectories from Ref. [32] are presented in Fig. 1. In fact, one of the 0^+2^{++} candidates is situated very close to the trajectory of $\mathbb{P}_2$.

In Ref. [32], this three-component Pomeron model was successfully used for the description of high-energy pp and $\bar{p}p$ data in the region of large momentum transfers, $0.01 \le |t| \le 14.5\ \text{GeV}^2$. In Ref. [26], the model was extended to the region of small momentum transfers,

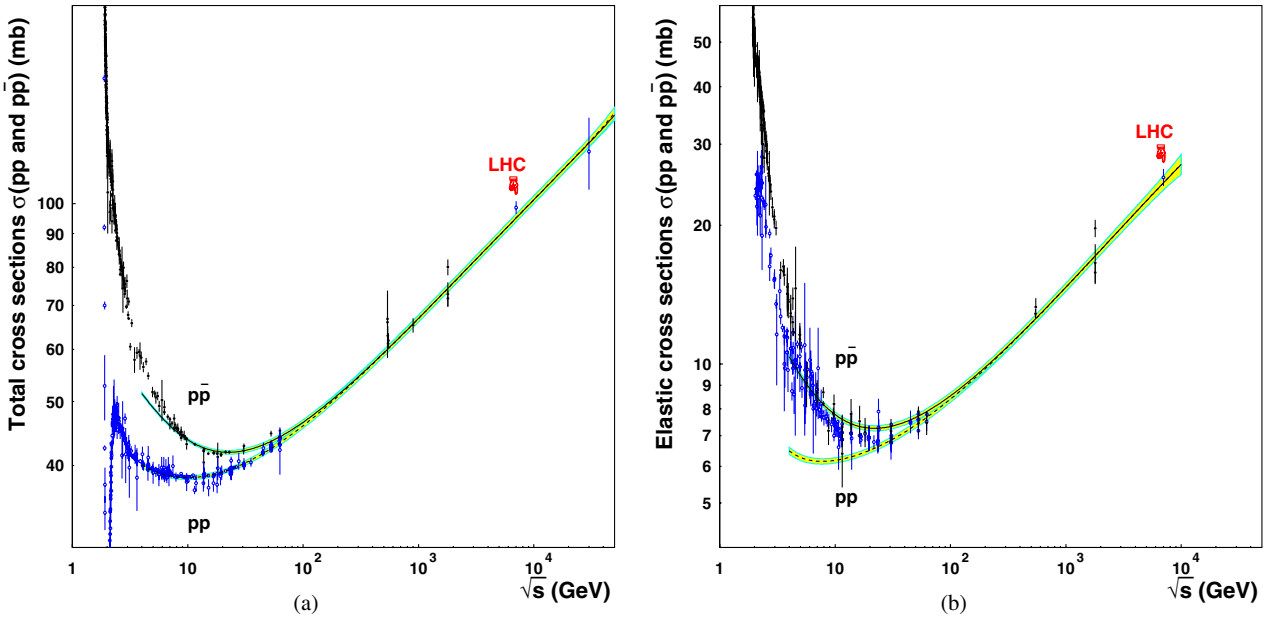

FIG. 2 (color online). Total (a) and elastic (b) cross sections for pp and $p\bar{p}$ scattering. The band corresponds to the error propagation of parameter uncertainties of the model.

$0 \leq |t| \leq 0.01$ GeV^2. In order to do this, we have to account for the Coulomb interaction. The standard way is to represent the whole scattering amplitude $T(s,t)$, which is dominated by the Coulomb force at low-momentum transfers and by the hadronic force at higher-momentum transfers, as

$$T(s,t) = T^N(s,t) + e^{i\alpha\Phi}T^C(s,t), \tag{4}$$

where we normalize the scattering amplitude so that

$$\frac{d\sigma}{dt} = \frac{|T(s,t)|^2}{16\pi s^2}, \tag{5}$$

and the Born Coulomb amplitude for pp and $\bar{p}p$ scattering is

$$T^C(s,t) = \mp\frac{8\pi\alpha s}{|t|}. \tag{6}$$

The upper (lower) sign corresponds to the scattering of particles with the same (opposite) charges. $T^N(s,t)$ stands for purely strong interaction amplitude, and the phase Φ depends generally on energy, momentum transfer, and the properties of T^N. We considered three different forms of the phase Φ calculated earlier by West and Yennie [42], Cahn [43], and Selyugin [44] and showed in Ref. [26] that all three phases lead to a good description of the low-t data.

In order to relate t and b spaces, one proceeds via Fourier-Bessel transforms:

$$\hat{f}(t) = 4\pi s\int_0^\infty db^2 J_0(b\sqrt{-t})f(b), \tag{7}$$

$$f(b) = \frac{1}{16\pi s}\int_{-\infty}^0 dt J_0(b\sqrt{-t})\hat{f}(t). \tag{8}$$

Crossing symmetry is restored by replacing $s \rightarrow se^{-i\pi/2}$. We introduce the dimensionless variable

$$\tilde{s} = \frac{s}{s_0}e^{-i\frac{\pi}{2}}, \qquad s_0 = 1\ (\text{GeV}^2), \tag{9}$$

in terms of which we give each $C+$ and $C-$ contribution with an appropriate signature factor in the form

$$\delta^{\pm}(s,b) = \mathcal{C}\frac{c}{s_0}\tilde{s}^{\alpha(0)-1}\frac{e^{-\frac{b^2}{\rho^2}}}{4\pi\rho^2}, \quad \text{with} \quad \rho^2 = 4\alpha'(0)\ln\tilde{s} + r^2, \tag{10}$$

where $\mathcal{C} = i$ for $C+$, and $\mathcal{C} = 1$ for $C-$.

For the cross sections, we use the following normalizations: Total and elastic cross sections are normalized such that

$$\sigma_{\text{tot}} = \frac{1}{s}\Im\text{m}T(s,t=0), \qquad \sigma_{\text{elastic}} = 4\pi\int_0^\infty db^2|T(s,b)|^2. \tag{11}$$

III. RESULTS AND DISCUSSIONS

In Ref. [32], the adjustable parameters were fitted over a set of 982 pp and $\bar{p}p$ data points [45] of both forward observables (total cross sections σ_{tot}, and ratios ρ of the real to the imaginary part of the amplitude) in the range $8 \leq \sqrt{s} \leq 1800$ GeV and angular distributions ($\frac{d\sigma}{dt}$) in the ranges $23 \leq \sqrt{s} \leq 1800$ GeV and $0.01 \leq |t| \leq 14$ GeV^2. A good χ^2/d.o.f. $= 2.6$ was obtained, and the parameters are given in Table II. (We did not consider systematic errors in normalizations of data sets, and thus assumed the value of χ^2/d.o.f. to be satisfactory.) A set of the data including the Coulomb region which consists of 2158 points [45] was considered in Ref. [26], and it was shown that Coulomb nuclear interference well described the data. We also found that the Coulomb phases from Ref. [43] and Ref. [44] gave a good account of the data in the lowest-t region.

The total and elastic cross sections are presented in Fig. 2. Note that, in contrast to Ref. [32], we included the error corridor as explained in the Appendix. In Fig. 2, we also plot the experimental values of the total and elastic cross sections found by the TOTEM Collaboration. As one can see, the model predictions are very close to the data. We show $p\bar{p}$ angular distributions over the full range of $|t|$ and in comparison with the D0 data at 1.96 TeV in Fig. 3. One can see that the data are predicted perfectly well by the model.

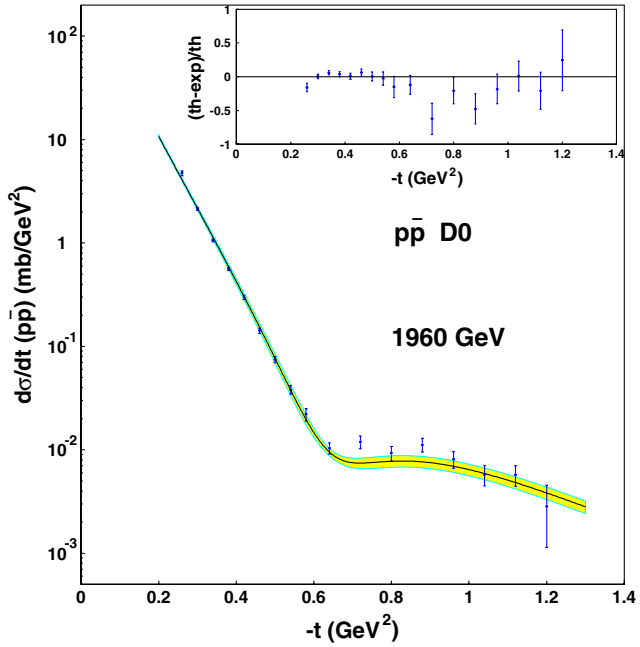

FIG. 3 (color online). Differential cross section for $p\bar{p}$ scattering at 1.96 TeV and comparison with the D0 data. The band corresponds to the error propagation of parameter uncertainties of the model. The upper panel shows the variance of the model predictions and the data.

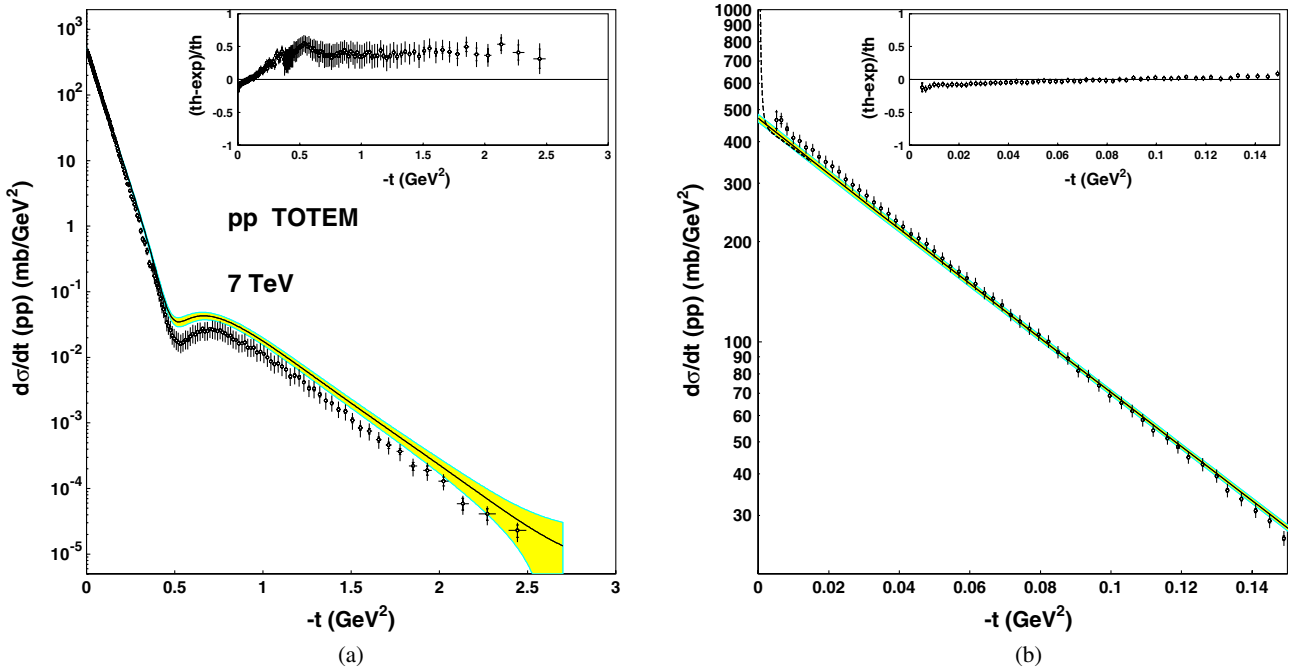

FIG. 4 (color online). Differential cross section for pp scattering at 7 TeV in comparison with the TOTEM data over the whole (a) and small-t (b) regions. The band corresponds to the error propagation of parameter uncertainties of the model. The upper panel shows the variance of the model predictions and the data. The cross section with Coulomb nuclear interference is shown by the dashed line in (b).

We show pp angular distributions over the full range of $|t|$ in comparison with the TOTEM data at 7 TeV in Fig. 4(a). Considering that the measurement spans 8 orders of magnitude, the match of the prediction and the measurements is fairly satisfactory. The model has some deviation from the data in the dip region, around $|t| \geq |t_{\rm dip}| = 0.52$ GeV^2; however, this region is the most subtle one, so we leave its description to a future analysis. In the small-t region [see Fig. 4(b)], the comparison of our predictions and the measured cross section remains fair, and the data and predictions differ by less than 10%. However, we must observe that the slope of the measured cross section is higher than our prediction [see Fig. 4(b)]. A comparison of predicted values and the ones measured by TOTEM is presented in Table I. One can see that the model predicts the general trend of the data quite well. There are, however, non-negligible deviations; in particular, the total cross section is slightly underestimated, and the slope of the elastic differential cross section and $d\sigma_{\rm el}/dt|_{t=0}$ are slightly smaller than measured values. The inelastic cross section at 7 TeV was measured by the TOTEM [2,4], CMS [5,6], ALICE [7], and ATLAS collaborations [8], while our model prediction is $\sigma_{\rm inelastic} = 70.34 \pm 2.11$ mb and $\sigma_{\rm inelastic}/\sigma_{\rm tot} = 0.74$ (see Table I).

TABLE I. Comparison of experimental measurements by the TOTEM [2,4], CMS [5,6], ALICE [7], and ATLAS collaborations [8] with model predictions [32] at $\sqrt{s} = 7$ TeV.

	Experimental result	Model prediction
$\sigma_{\rm tot}$ [mb], TOTEM, [4]	98.58 ± 2.23	95.06 ± 1.26
$\sigma_{\rm elastic}$ [mb], TOTEM, [4]	25.42 ± 1.07	24.72 ± 0.85
$\sigma_{\rm inelastic}$ [mb], TOTEM, [3]	$73.5 \pm 0.6^{+1.8}_{-1.3}$	70.34 ± 2.11
$\sigma_{\rm inelastic}$ [mb], CMS, [6]	$64.5 \pm 3.0 \pm 1.5$	70.34 ± 2.11
$\sigma_{\rm inelastic}$ [mb], CMS, [5]	$68 \pm 2 \pm 2.4 \pm 4$	70.34 ± 2.11
$\sigma_{\rm inelastic}$ [mb], ATLAS, [8]	$69.4 \pm 2.4 \pm 6.9$	70.34 ± 2.11
$\sigma_{\rm inelastic}$ [mb], ALICE, [7]	$73.2^{+2.0}_{-4.6} \pm 2.6$	70.34 ± 2.11
$d\sigma_{\rm el}/dt\|_{t=0}$ [mb/GeV^2], TOTEM, [4]	506.4 ± 23.0	470.9 ± 12.5
B [mb/GeV^2] [GeV^{-2}], TOTEM, [4]	19.89 ± 0.27	19.32
$B_{(\lvert t\rvert=0.4\ \rm GeV^2)}$ TOTEM, [GeV^{-2}], [2]	$23.6 \pm 0.5 \pm 05$	22.1
$\lvert t_{\rm dip}\rvert$ [GeV^2], TOTEM, [2]	$0.53 \pm 0.01 \pm 0.01$	0.52

TABLE II. Parameters obtained in Ref. [32].

Pomeron_1	Odderon
$\Delta_{\mathbb{P}_1} = 0.0578 \pm 0.0020$	$\Delta_{\mathbb{O}} = 0.19200 \pm 0.0025$
$c_{\mathbb{P}_1} = 53.007 \pm 0.795$	$c_{\mathbb{O}} = 0.0166 \pm 0.0022$
$\alpha'_{\mathbb{P}_1} = 0.5596 \pm 0.0078\ (\text{GeV}^{-2})$	$\alpha'_{\mathbb{O}} = 0.048 \pm 0.0027\ (\text{GeV}^{-2})$
$r^2_{\mathbb{P}_1} = 6.3096 \pm 0.2522\ (\text{GeV}^{-2})$	$r^2_{\mathbb{O}} = 0.1398 \pm 0.0570\ (\text{GeV}^{-2})$
Pomeron_2	ω-Reggeon
$\Delta_{\mathbb{P}_2} = 0.1669 \pm 0.0012$	$\Delta_\omega = -0.53$ (FIXED)
$c_{\mathbb{P}_2} = 9.6762 \pm 0.1600$	$c_\omega = -174.18 \pm 2.72$
$\alpha'_{\mathbb{P}_2} = 0.2733 \pm 0.0056\ (\text{GeV}^{-2})$	$\alpha'_\omega = 0.93\ (\text{GeV}^{-2})$ (FIXED)
$r^2_{\mathbb{P}_2} = 3.1097 \pm 0.1817\ (\text{GeV}^{-2})$	$r^2_\omega = 7.467 \pm 1.083\ (\text{GeV}^{-2})$
Pomeron_3	f-Reggeon
$\Delta_{\mathbb{P}_3} = 0.2032 \pm 0.0041$	$\Delta_f = -0.31$ (FIXED)
$c_{\mathbb{P}_3} = 1.6654 \pm 0.0669$	$c_f = 191.69 \pm 2.12$
$\alpha'_{\mathbb{P}_3} = 0.0937 \pm 0.0029\ (\text{GeV}^{-2})$	$\alpha'_f = 0.84\ (\text{GeV}^{-2})$ (FIXED)
$r^2_{\mathbb{P}_3} = 2.4771 \pm 0.0964\ (\text{GeV}^{-2})$	$r^2_f = 31.593 \pm 1.099\ (\text{GeV}^{-2})$

This ratio is close to its experimental value, $\sigma_{\text{inelastic}}/\sigma_{\text{tot}} \approx 0.72$.

Given the quality of the comparison, we are confident that, on the whole, our model has proved its predictive power. Detailed analysis of the impact of the TOTEM data on the parameters of the model will be presented elsewhere.

IV. CONCLUSIONS

The above analysis shows that the D0 data [1] on the total and differential cross sections support our predictions. Total, elastic, and inelastic cross-section predictions are in agreement with the measurements by TOTEM [2,4], CMS [5,6], ALICE [7], and ATLAS [8]. The TOTEM [4] results on the differential elastic cross section, while being in agreement with the predictions of such general characteristics as the forward slope and the position of the dip, reveal a moderate but non-negligible discrepancy with the observed t dependence at large t. Nonetheless, the disagreement with the TOTEM data [4] is, to our mind, far from being deadly. We believe that the model should be improved, as—for example—in view of possible future measurements of the diffractive central production of Higgs and other states, there is a need for a good model of diffraction, whose parameters constitute an important element of the corresponding modeling. We must also add that the very model contains, in its theoretical framework, a lot of potential sources for further refinement. It would also be very helpful if the TOTEM data on differential cross sections would be supplemented by some other independent measurements at the LHC.

ACKNOWLEDGMENTS

We are grateful to Roman Ryutin and Anton Godizov for useful discussions of the subject of this paper, and to Michael Pennington for critical reading of the manuscript. This paper was authored by a Jefferson Science Associate, LLC, under U.S. DOE Contract No. DE-AC05-06OR23177. The U.S. government retains a nonexclusive, paid-up, irrevocable, worldwide license to publish or reproduce this manuscript for U.S. government purposes.

APPENDIX

In order to estimate the error corridor of our predictions from Ref. [32], we use the following method: Generically, for a measured function $f(x, \{a\})$ that depends on variable x and a set of parameters $\{a\} = \{a_1, \ldots, a_N\}$, error propagation reads

$$(\Delta f(x, \{a\}))^2 = \sum_{i=1}^{N} \sum_{j=1}^{N} C_{ij} \frac{\partial f}{\partial a_i} \sigma_i \frac{\partial f}{\partial a_j} \sigma_j, \tag{A1}$$

where σ_i, σ_j are one-sigma errors on parameters (in our case, we use those from Table II) and C_{ij} is the correlation coefficient for the parameters i and j. For totally uncorrelated parameters, we have $C_{ij} = \delta_{ij}$, and the formula reduces to the standard one:

$$(\Delta f(x, \{a\}))^2 = \sum_{i=1}^{N} \left(\frac{\partial f}{\partial a_i} \right)^2 \sigma_i^2. \tag{A2}$$

We extract the error correlation matrix from Ref. [32] and apply Eq. (A1) to all measured quantities plotted in this paper.

[1] V. M. Abazov *et al.* (D0 Collaboration), Phys. Rev. D **86**, 012009 (2012).
[2] G. Antchev *et al.* (TOTEM Collaboration), Europhys. Lett. **95**, 41001 (2011).
[3] G. Antchev, P. Aspell, I. Atanassov, V. Avati, J. Baechler, V. Berardi, M. Berretti, E. Bossini *et al.*, Europhys. Lett. **96**, 21002 (2011).
[4] G. Antchev, P. Aspell, I. Atanassov, V. Avati, J. Baechler, V. Berardi, M. Berretti, E. Bossini *et al.*, CERN Report No. CERN-PH-EP-2012-239, 2012.
[5] CMS Collaboration, CMS Report No. CMS-PAS-FWD-11-001, 2011.
[6] CMS Collaboration, CMS Report No. CMS-PAS-QCD-11-002, 2011.
[7] B. Abelev *et al.* (ALICE Collaboration), arXiv:1208.4968.
[8] G. Aad *et al.* (ATLAS Collaboration), Nat. Commun. **2**, 463 (2011).
[9] C. Bourrely, J. M. Myers, J. Soffer, and T. T. Wu, Phys. Rev. D **85**, 096009 (2012).
[10] J. Soffer, arXiv:1206.3657.
[11] A. Grau, S. Pacetti, G. Pancheri, and Y. N. Srivastava, Phys. Lett. B **714**, 70 (2012).
[12] O. V. Selyugin, Eur. Phys. J. C **72**, 2073 (2012).
[13] F. Nemes and T. Csorgo, Int. J. Mod. Phys. A **27**, 1250175 (2012).
[14] C. Merino and Y. M. Shabelski, J. High Energy Phys. 05 (2012) 013.
[15] A. A. Godizov, arXiv:1203.6013.
[16] M. G. Ryskin, A. D. Martin, and V. A. Khoze, Eur. Phys. J. C **72**, 1937 (2012).
[17] V. A. Schegelsky and M. G. Ryskin, Phys. Rev. D **85**, 094024 (2012).
[18] A. I. Lengyel and Z. Z. Tarics, arXiv:1206.5837.
[19] S. M. Troshin and N. E. Tyurin, Mod. Phys. Lett. A **27**, 1250111 (2012).
[20] E. Gotsman, E. Levin, and U. Maor, Phys. Rev. D **85**, 094007 (2012).
[21] M. M. Block and F. Halzen, arXiv:1201.0960.
[22] A. Donnachie and P. V. Landshoff, arXiv:1112.2485.
[23] B. Z. Kopeliovich, I. K. Potashnikova, and B. Povh, Phys. Rev. D **86**, 051502 (2012).
[24] M. M. Block and F. Halzen, Phys. Rev. Lett. **107**, 212002 (2011).
[25] M. M. Block and F. Halzen, Phys. Rev. D **86**, 051504 (2012).
[26] V. A. Petrov, E. Predazzi, and A. Prokudin, Eur. Phys. J. C **28**, 525 (2003).
[27] M. M. Block and F. Halzen, Phys. Rev. D **83**, 077901 (2011).
[28] C. Bourrely, J. Soffer, and T. T. Wu, Eur. Phys. J. C **28**, 97 (2003).
[29] M. M. Islam, J. Kaspar, and R. J. Luddy, Mod. Phys. Lett. A **24**, 485 (2009).
[30] L. Jenkovszky, O. Kuprash, J. Lamsa, and R. Orava, Mod. Phys. Lett. A **26**, 2029 (2011).
[31] J. Kaspar, V. Kundrat, M. Lokajicek, and J. Prochazka, Nucl. Phys. **B843**, 84 (2011).
[32] V. A. Petrov and A. V. Prokudin, Eur. Phys. J. C **23**, 135 (2002).
[33] C. Lovelace, Nucl. Phys. **B95**, 12 (1975); D. Heckathorn, Phys. Rev. D **18**, 1286 (1978); L. N. Lipatov, Sov. Phys. JETP **63**, 904 (1986).
[34] O. V. Kancheli, arXiv:1105.0792.
[35] A. A. Godizov, Phys. Rev. D **81**, 065009 (2010).
[36] N. N. Nikolaev, Nucl. Phys. B, Proc. Suppl. **12**, 95 (1990).
[37] A. Donnachie and P. V. Landshoff, Phys. Lett. B **437**, 408 (1998).
[38] A. K. Likhoded and O. P. Yushchenko, Int. J. Mod. Phys. A **06**, 913 (1991).
[39] J. Ellis, H. Kowalski, and D. A. Ross, Phys. Lett. B **668**, 51 (2008).
[40] V. A. Petrov, AIP Conf. Proc. **1105**, 266 (2009); A. A. Godizov and V. A. Petrov, J. High Energy Phys. 07 (2007) 083.
[41] R. Kirschner and L. N. Lipatov, Z. Phys. C **45**, 477 (1990).
[42] G. B. West and D. R. Yennie, Phys. Rev. D **172**, 1413 (1968).
[43] R. Cahn, Z. Phys. C **15**, 253 (1982).
[44] O. V. Selyugin, Phys. Rev. D **60**, 074028 (1999).
[45] The data are available at the Reaction Data Database, http://durpdg.dur.ac.uk/hepdata/reac.html.